Recyclability of ceramic powder in CerAM vat photopolymerization

Open Ceramics 25 (2026) 100908

Contents lists available at ScienceDirect

Open Ceramics

journal homepage: www.sciencedirect.com/journal/open-ceramics

Recyclability of ceramic powder in CerAM vat photopolymerization

Matilde Aronne [a,*], Eric Schwarzer-Fischer [b], Alberto Ballesio [a,c], Nadine Lorenz [b], Valentina Bertana [a], Uwe Scheithauer [b], Sergio Ferrero [a], Luciano Scaltrito [a]

[a] CHILAB-ITEM Interfacing Technologies for Edge Microsystems, Department of Applied Science and Technology (DISAT), Politecnico di Torino, Via Lungo Piazza d'Armi 6, 10034 Chivasso, Italy
[b] Fraunhofer Institut für Keramische Technologien und Systeme (IKTS), Winterbergstraße 28, 01277 Dresden, Germany
[c] CNR-IMEM, Parco Area delle Scienze 37/A, 43124 Parma, Italy

ARTICLE INFO

Keywords:
CerAM VPP
Recycling
Sustainability
Alumina DLP
Additive manufacturing

ABSTRACT

The sustainability of the manufacturing industry is becoming an increasingly hot topic, particularly the reintroduction of waste into the production chain. The use of AM of ceramics can reduce waste and enable complex, lightweight designs, however, practical routes to circularity remain underdeveloped. This investigation aims to explore the potential of coupling these additive fabrication techniques with raw materials from alternative sources of ceramics, such as printing wastes and error prints, developing a photocurable ceramic suspension for DLP technology. For resin preparation, a polymeric premix was first prepared by combining a mixture of different acrylate monomers as a photoreactive binder with a non-reactive plasticizing additive. Alumina was recovered from failed green bodies following matrix burning out, parts grinding and sieving of the obtained powder. Subsequent investigations of the powder by SEM imaging and EDX analysis were carried out to verify particle morphology and average dimensions and to identify any contaminants in the recycled material. The suspension viscosity and curing behaviour were measured. Finally, the mechanical characteristics of printed parts, their density, their shrinkage, as well as possible contaminants, were evaluated, in order to understand the impact of the recycling process on material performances and to determine its possible application fields. Tests results provided a practical recycling potential for alumina in DLP, offering viable solutions in facilitating closed-loop CerAM manufacturing.

1. Introduction

Ceramic materials have attracted increased interest for their use in additive manufacturing (AM) technologies. Ceramic AM (CerAM) technologies refer to a broad range of manufacturing strategies that rely on the deposition of material layer by layer, through different techniques like photopolymerization or extrusion-based ones. A short overview of the possible CerAM technologies is reported in Fig. 1 below.

CerAM vat photopolymerization (VPP) technologies include all fabrication processes based on a photocurable resin that is shaped in the final form through a light source, layer-by-layer. These techniques ensure high resolution, high surface quality and finishing, with a good reproducibility. This has led to a significant increase in the level of interest surrounding these fabrication technologies [2]. VPP technologies are divided into two categories, based on the light source:

- Ceramic Stereolithography (SL), that relies on a vat of photocurable resin which is cured point-by-point, layer-by-layer, through a laser source. The thin layer of liquid resin is solidified by the laser source, that can be positioned above or below the vat, so the building platform is positioned consequently using a top-down approach or a bottom-up one. Movements in x- y- plane are done by the laser, while in the z- axis the movement is guaranteed by the building platform up and down stages [3].
- Ceramic Digital light projector (DLP), that relies on a vat of photocurable resin which is cured layer-by-layer through a UV projector. The difference with SL approach is that the resin is exposed to the UV light source through a pattern mask, that is represented by a digital micromirror device, with high reflectivity, contrast and resolution. The number of micromirrors is equal to the number of pixels that switch between on or off to produce the desired image. The remaining elements, such as the vat, the building platform, and the moving system, remain consistent with those of SL technology [4].

* Corresponding author.
E-mail address: matilde.aronne@polito.it (M. Aronne).

https://doi.org/10.1016/j.oceram.2026.100908
Received 26 October 2025; Received in revised form 4 December 2025; Accepted 1 January 2026
Available online 2 January 2026

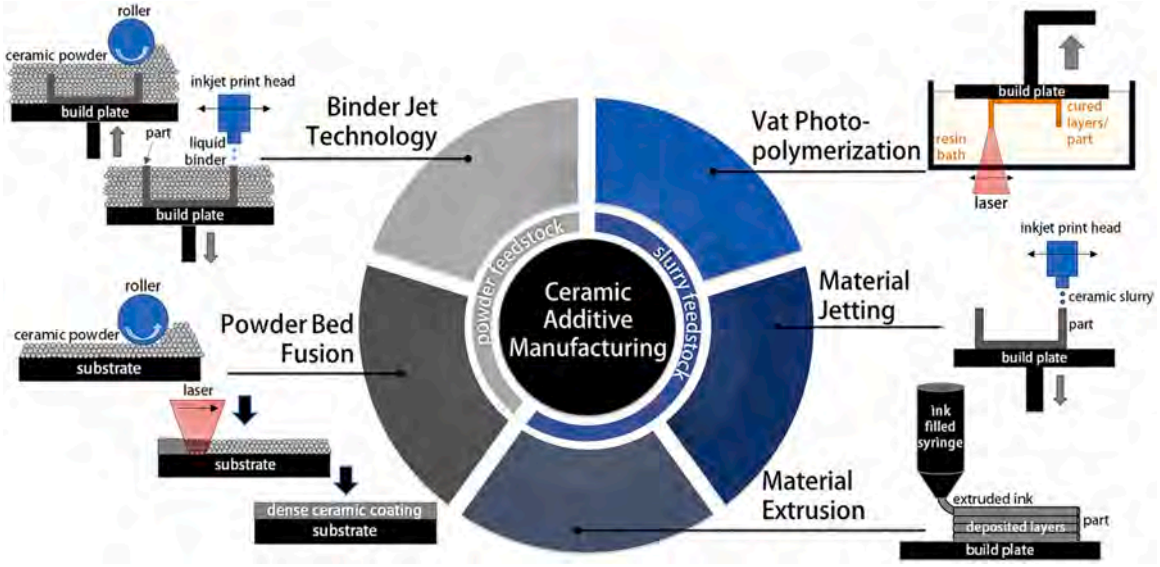

Fig. 1. CerAM technologies, divided by their technical differences and feedstock materials. Reprinted from Journal of the American Ceramic Society, vol. 107, J. Kaufman, J. O. Hardin, L. A. Baldwin, et al, "Future directions in ceramic additive manufacturing: Fiber reinforcements and artificial intelligence", 2023, with permission from John Wiley and Sons [1].

Application fields of these technologies range from biomedical field to aerospace, due to their advantages. Biomedical sector, like dentistry, implantology and so on, rely more and more on the use of VPP technologies for personalized solutions. CerAM SL and DLP can help in dental restoration, as crown fabrication, thanks to the high level of precision and reproducibility.

Another field of application for CerAM VPP technologies is energy, where materials like oxides, silicates, perovskites, spinel are chosen for their electrical, thermal and magnetic properties [5]. Energy and electronic related field of application for CerAM technologies and materials is fabrication of heat exchanger. These devices are used for collecting heat generated from a source, i.e. electronic device, and transferring it to another, which can be a second device or a fluid [5]. A DLP based approach was used by Schwarzer-Fischer et al. [6] for fabricating a AlN heat sink. The material ensured high thermal conductivity and high dielectric properties, making them suitable for heat exchange applications. It was well shaped through CerAM VPP technology, realizing a component with complex inner design, like cooling channels, that showed excellent thermal behaviour [6]. Important application field for ceramics is aerospace, due to materials stability, both chemical and dimensional, thermal resistance, corrosion resistance, and low density, compared to metals, that help in lightweighting of parts and reducing fuel consumption. Both oxide and non- oxide ceramics are used in the field, because oxides can guarantee good reactivity, leachability, processability, phase stability with temperature increase, as well as the required flexural strength. Non-oxides like SiC are more and more investigated in aerospace sector, because of its greater strength, higher chemical stability with temperature increase, higher thermal conductivity and wear resistance. However, it is difficult to suspend this type of materials in photocurable resins, a lot of researchers are focusing on the optimization of suspension preparation and sintering [2].

The interest in coupling CerAM with several application fields is enormous, to save costs, to fabricate complex shapes in shorter time, to guarantee design flexibility in device prototyping, to enable mass customization, and to work with more materials in one fabrication step, thanks to new multi-materials CerAM VPP technologies [7]. However, these are not the only benefits provided by the application of AM technologies to ceramic manufacturing field. These fabrication techniques show characteristics that make them more sustainable than traditional subtractive ones. Several works focused on potentiality of AM technologies for reducing devices fabrication impact. The review of Hegab et al. [8] explained how AM can provide some benefits that make AM technologies more environmentally friendly than traditional techniques. As emerged from this work, the environmental benefits in the application of AM technologies can be summarized as follow:

- Less material required for printing, that means reduction in raw material consumption.
- Reduction in emissions and wastes, that means fewer polluting processes.
- Allow for delocalization of product manufacturing, closer to final users, eliminating the need for transportation.

Furthermore, these fabrication processes seem to be more suitable for repair and remanufacturing of defective/damaged tools, eliminating the need for manufacturing new tools and shortening the supply chain.

As presented by [9], environmental sustainability of AM technologies is also related to the reduction in overproduction, that is correlated with the free form design of 3D printed devices and customization. Printing customized and modified parts decrease the need for mass production, as well as the probability of surplus goods [9]. How to combine the need for sustainable design and fabrication processes was exposed in [10]. They introduced the concept of eco-design, which involve the environmental impact evaluations all over the design and manufacturing chain. An optimize design can provide economic and social benefits too, which make AM technologies sustainable in general sense. These optimizations processes that involve economic, social and environmental sustainability are part of the so-called triple bottom line (TBL) [10]. Economical aspect of sustainability in the use of AM technologies are mostly related to reduction of material usage, produced items, and no need for tools and moulds fabrications, because these are the aspects that require higher expenses [8]. Concerning the social aspect of AM technologies sustainability, there is a lack in literature about this topic, as stated by Jayawardane et al. [11], even if these technologies are gaining ground in industry scale production too. However, researchers underlined the need for further evaluations of AM materials, for better understanding the potential new issues correlated to organic chemical emitted substances during AM fabrication processes [8].

Considering the possibility of AM for sustainable design, what seems to be applicable is the introduction of recycled materials in the process chain. This implementation of one pillar of circular economy (CE)

Table 1
Composition of the polymeric premix for alumina-based resin for DLP.

Name	Percentage	Brand	Function
Polypropylene Glycol (PPG400)	6 %wt	Sigma-Aldrich by Merck, Darmstadt, Germany	Plasticizing fluid
Ebecryl 83	5.61 %wt	BASF Ludwigshafen, Germany	Monomer
Laromer 8887	8.40 %wt	BASF Ludwigshafen, Germany	Linker
Camphorquinone	0.064 %wt	Sigma-Aldrich by Merck, Darmstadt, Germany	Photoinitiator
Ethyl 4-Dimethylaminobenzoate	0.075 %wt	Fischer Scientific GmbH, Schwerte, Germany	Co-initiator
Solsperse 85000	0.7 %wt	Lubrizol Deutschland GmbH, Hamburg, Germany	Dispersant

concept was already exposed in polymers AM world, because several researchers have already started to prototype devices from recycled materials. The motivation to engage in research on this subject is derived from the idea that AM and CE together have a synergic effect of giving new life and value to wastes [12]. Even if mostly of the research about recycling of materials through AM technologies are focused on polymers, new studies about metals and ceramics recycling in AM field are rising nowadays [10]. This interest in materials recycling is pushed by not only environmental concerns, but also by other factors. Considering ceramics production, extraction and purification costs for consumer goods like alumina are comparable to the incomes [13,14], because of increasing raw materials costs and final product elevated availability on the market. Another reason behind ceramics recycling interest is related to electrical and thermal energy requirements, due to the big energy wasting generated during ceramic materials synthesis, shaping and post processing. Recycling can help in reducing the energy consumption for powder synthesis, which is beneficial for the ceramic sector energy requirements. However, further evaluation on energy requirements for ceramics recycling should be undertaken, considering that is also possible to reduce the amount of energy for disposing ceramic wastes. Furthermore, coupling greener energy sources with recycling processes can better influence the supply chain, reducing the environmental impact of the whole system [15]. Lastly, regulatory agencies, both at national and international levels, are more and more interested in the disposal and management of ceramic wastes, their reuse in different sector or recycling in the original one, with the final aim of reducing emission and resources exploitation [16]. Because of a lack in methodologies for best practices in recycling of ceramics, researchers and industry are looking for solutions to accomplish the goal.

In this perspective, the aim of this work is to introduce a possible protocol for Al_2O_3 powder recovering and reusing in CerAM VPP technology. Alumina powder was recovered from DLP printed alumina parts that showed defects on the surface or failed during the print job. The polymeric residues were eliminated through a thermal treatment, then agglomerates were manually grinded, and the collected powder was sieved. Finally, recycled Al_2O_3 was dispersed in a photocurable resin for DLP printing. Several material and parts characterizations were performed: alumina powder morphology and composition were checked through scanning electron microscopy (SEM), energy dispersive X-ray analysis (EDX), resonance frequency analysis (RFA). Suspension rheology and light response was evaluated through viscosity measurement and curing depth test. Printed and sintered bodies were shaped according to the parts tests performed: density evaluation, linear shrinkage and mechanical behaviour (following CharAM methodology [17,18]).

2. Materials and methods

2.1. Material preparation

2.1.1. Powders

The starting material for Al_2O_3 recovering was AES11c alumina powder from (purity 99.7 %, Sumitomo Chemical Tokyo, Japan), firstly used as filler for a DLP resin. Failed printed parts and damaged green bodies made of this suspension were first thermally treated, using a furnace (ARCA 20, Schütz Dental GmbH, Rosbach, Germany). Then, all the components were heated up to 600 °C for 8 h, with a heating rate of 3 K/min. Subsequentially, treated parts were manually grinded using a mortar and pestle, to destroy any agglomerates present, then powder was sieved using a standard 100 μm sieve, for a first removal of bigger grains that severely impede the reaching of the minimum printed dimension desired. This material recycling protocol was applied not only to printing errors and damaged green bodies made of initial Al_2O_3 suspension, but it was also applied to printed parts made of one-time recycled alumina, to verify if any decrease of performance was registered and since which recycling cycle. The recovered powder was then analyzed to identify any possible particle agglomeration left and contaminants, so SEM microscopy (SUPRA™ 40 from ZEISS, Oberkochen, Germany) was performed for particles morphology evaluation, while EDX (Oxford EDS microanalysis, Liquid-N2 cooled Si(Li) detector, Oxford Instruments, Abingdon, United Kingdom) was carried out for composition assessment. For particles size measurement, ImageJ 1.54 g software was used.

2.1.2. Resin

79 %wt. of Al_2O_3 powder, both initial and recycled one, was used as filler for a DLP resin, whose composition is reported in the Table 1 below.

For dispersing the solid part into the polymeric premix, a planetary centrifugal vacuum mixer (Thinky ARV-310, C3 Prozess- und Anlagensentechnik, Haar, Germany) was used. The parameters for mixing were divided into several steps. Firstly, the plasticizer and monomer were mixed for 5 min at 2000 rpm, then the same mixing stage was repeated two times, one for the addition of the linker, then for the addition of photoinitiators. After each mixing phase, a cooling down step of few minutes was performed. Later, the premixed suspension was further mixed with the dispersant for 1 min at 2000 rpm. Lastly, the polymeric mix and the powder were homogenously mixed through 4 steps of 1 min at 2000 rpm, alternating with 10 min cooling down phases. To better understand the influence of this mixing step on the final mechanical characteristics of printed parts, an additional mixing phase was added, using a homogenizer (DISPERMAT CA 20-C, VMA-GETZMANN GMBH, Reichshof, Germany). Polymeric premix was homogenized with the powders for 4 h at 1000 rpm, using a cooling liquid system to avoid suspension polymerization because of temperature. The aim of this step was to disrupt any residual agglomerate in the final suspension that could cause a reduction in mechanical performance. The prepared resins with initial powder, one-time recycled powder and two-time recycled powder, mixed with and without the homogenizer, were used for rheological behavior evaluation, using MCR 302 modular rheometer from Anton Paar (Graz, Austria). Measures were performed in a shear rates range of 0.01 to 1000 s^{-1}, to verify is the resin presented a shear thinning behaviour, with viscosity values below 80 Pa*s in the selected range [19]. Curing depth measurements were performed using the DLP projector at selected energy doses and measuring the thickness of one exposed layer reached by the light. For layer thickness measurement, a digital micrometre (High-Accuracy 13 Digimatic® Digital Micrometer) was used.

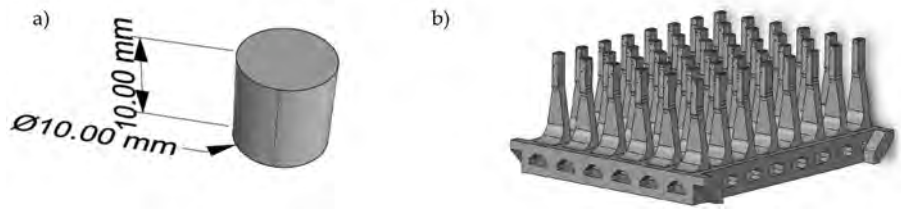

Fig. 2. CAD design of a) cylinders for density and shrinkage evaluation; b) CharAM test specimen - methodology for testing of mechanical performances [18].

Table 2
Major printing parameters, divided by powder sources used as filler for the DLP resin.

Parameters	Initial powder	One-time recycled powder	Two-time recycled powder
Layer Thickness	25 μm /50 μm	25/50 μm	50 μm
Exposure energy	150 mJ/cm^2 (1 layer) – 140 mJ/cm^2 (2-5 layers) – 130 mJ/cm^2	180 mJ/cm^2 (1 layer) – 170 mJ/cm^2 (2-5 layers) – 160 mJ/cm^2	180 mJ/cm^2 (1 layer) – 170 mJ/cm^2 (2-5 layers) – 160 mJ/cm^2
Light intensity	50 mW/cm^2	50 mW/cm^2	50 mW/cm^2
Vat rotation speed	200 rpm	200 rpm	200 rpm

2.2. Material shaping and white body manufacturing

2.2.1. CerAM VPP printing technology

The prepared resins were printed using a DLP based 3D printer CeraFab 8500 from Lithoz GmbH (Vienna, Austria). The machine relies on a rotational vat, where a recoater continuously mixes the material and spread a thin layer of photocurable resin. After that, the building platform goes down, reaching the desired distance from the vat bottom, that is the selected layer thickness. The projector is then turned on, projecting the layer geometry and triggering the material curing. To ensure a better diffusion of material in the vat, it tilts a little during the exposure, according to the tilt speed and angle indicated. Exposure time and vat rotational parameters were derived from curing depth evaluation and viscosity measurement, while the layer thickness was chosen based on the different geometries printed. Layer thicknesses used were 25 μm and 50 μm, based on the z resolution required for printing geometry A (Fig. 2a) or geometry B (Fig. 2b and Fig. 4).

The selected printing parameters were set based on the resins measured curing depth and viscosity. For resin with initial powder as filler, the layer thickness was selected according to the printed geometry and testing technology requirements, so for CharAM methodology, layer thickness should be 25 μm, while for cylinders, layer thickness was set at 50 μm. The exposure energy was 150 mJ/cm^2, for first layer, 140 mJ/cm^2, for the subsequent layer 5 layers, and 130 mJ/cm^2 for the rest of the job. The selected intensity was 50 mW/cm^2, while the vat rotation speed was 200 rpm. For the resin with one time recycled powder as filler, the layer thickness was selected according to the mixing stages used during preparation, so for the resin mixed only by the mixer, layer thickness was 50 μm, while for resin mixed with homogenizer, layer thickness was set at 25 μm for initial powder and 25 μm/ 50 μm for one-time recycled powder. The exposure energy was 180 mJ/cm^2, for first layer, 170 mJ/cm^2, for the subsequent layer 5 layers, and 160 mJ/cm^2 for the rest of the job, according to curing depth evaluation. The selected intensity was 50 mW/cm^2, while the vat rotation speed was 200 rpm. Lastly, for resin with two-time recycled alumina as filler, the layer thickness was set as 50 μm both for cylinders and CharAM samples, while the selected intensity was 50 mW/cm^2 and the vat rotation speed was 200 rpm, as for the other print jobs. The exposure energy was 180

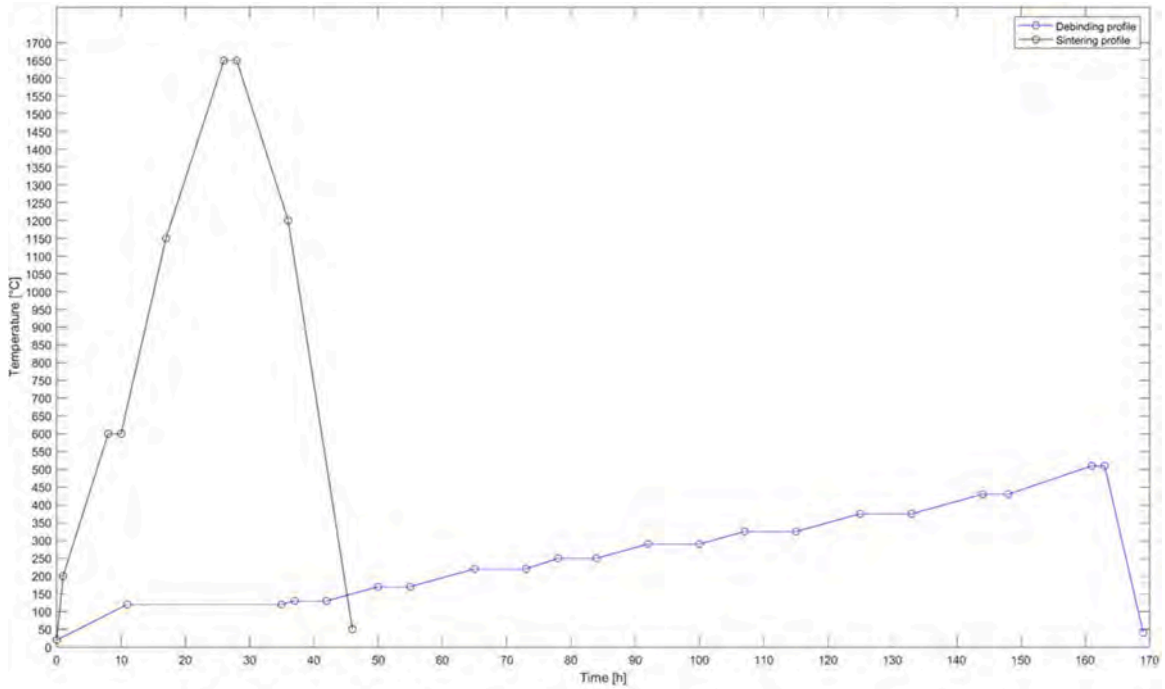

Fig. 3. Debinding profile (in blue) and sintering profile (in black), used for this work.

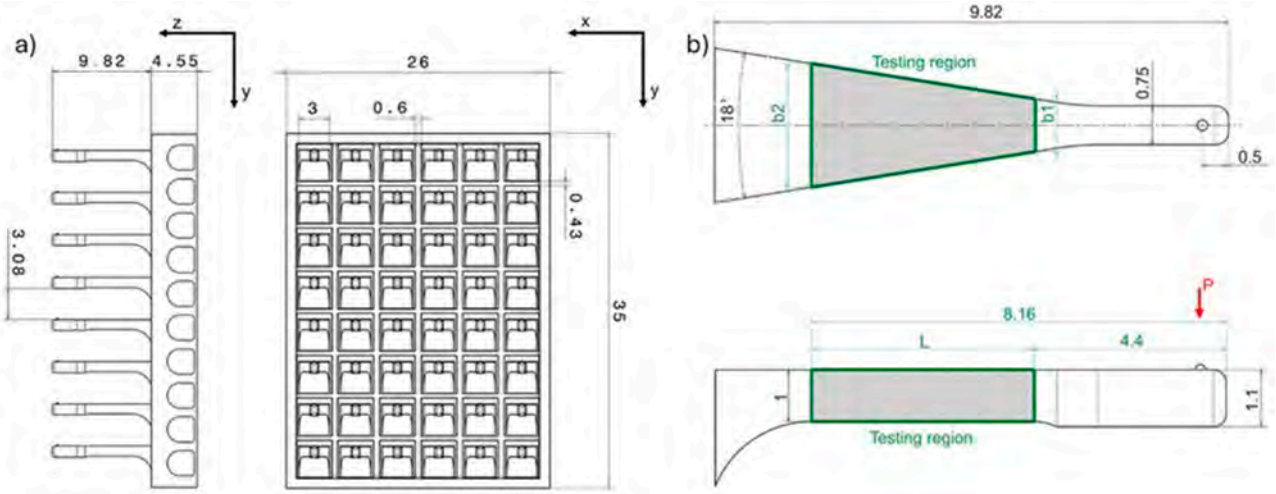

Fig. 4. Representation of the most significant dimensions, in mm, for the whole testing sample (in a) and for one cantilever (in b), where the testing region is highlighted, and the applied force direction is reported. Reprinted from [18].

mJ/cm^2, for first layer, 170 mJ/cm^2, for the subsequent layer 5 layers, and 160 mJ/cm^2 for the rest of the job, according to curing depth evaluation. A summary of the set parameters is reported in the Table 2 below.

2.2.2. Green and sintered body

Parts fabricated through CerAM technologies have to be thermally treated to obtain the final dense part. First thermal treatment is debinding, whose aim is to remove the organic binder from the green body [20]. In this work, debinding was performed in a furnace, relying on an inert nitrogen atmosphere for smoother debinding. The temperature profile for this step was composed of 13 steps, with different heating rates and dwell times (Fig. 3).

After debinding stage, the obtained brown bodies were sintered to densify the parts and obtain the final white body. This step temperatures are crucial for grains boundaries interconnection, influencing the microstructure and properties of the final object [21]. The sintering profile used for this work is reported in the table below (Fig. 3):

2.3. Samples characterizations

Final dense bodies were used to perform several characterizations. Firstly, 10 mm-by-10 mm cylinders were used for density evaluation through Archimedes' principle. The samples were submerged in distilled water overnight, then all air residues inside the samples were removed thanks to a vacuum pump. Lastly, density and open porosities were measured, weighting the samples in different conditions. The mentioned cylindrical geometry was also used for linear shrinkage evaluation, measuring the as printed and sintered diameter and height of the samples.

Another important element to consider is the mechanical behaviour of one-time and two-time recycled materials, compared to initial powder. For testing their performances, samples with the geometry (Fig. 2b) were undergone to CharAM technique, which helps in determining flexural strength using one testing sample made of several cantilever instead of the numerous samples needed for traditional mechanical tests like four point bending [17,18].

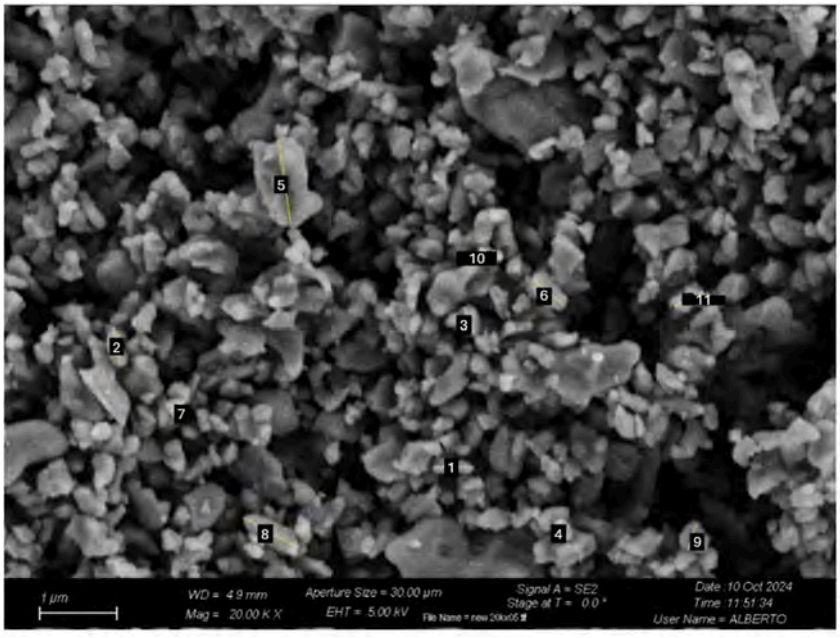

Label	Length (µm)
1	0,495
2	0,504
3	0,323
4	0,292
5	1,054
6	0,487
7	0,255
8	0,773
9	0,343
10	0,283
11	0,466

Fig. 5. SEM image of initial powder, with relative measurements.

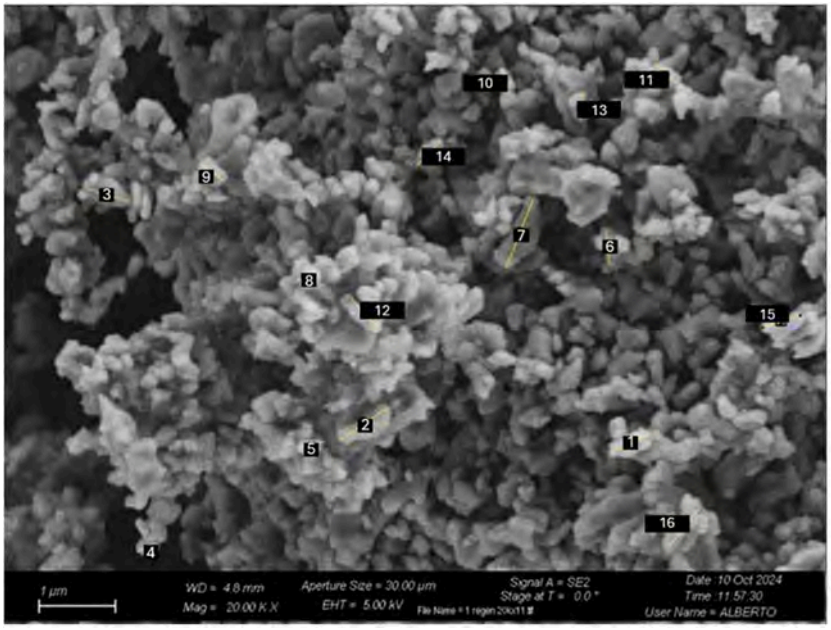

Label	Length (µm)
1	0,539
2	0,796
3	0,619
4	0,274
5	0,359
6	0,454
7	0,97
8	0,274
9	0,4
10	0,318
11	0,388
12	0,556
13	0,366
14	0,464
15	0,62
16	0,52

Fig. 6. SEM image of one-time recycled powder, with relative measurements.

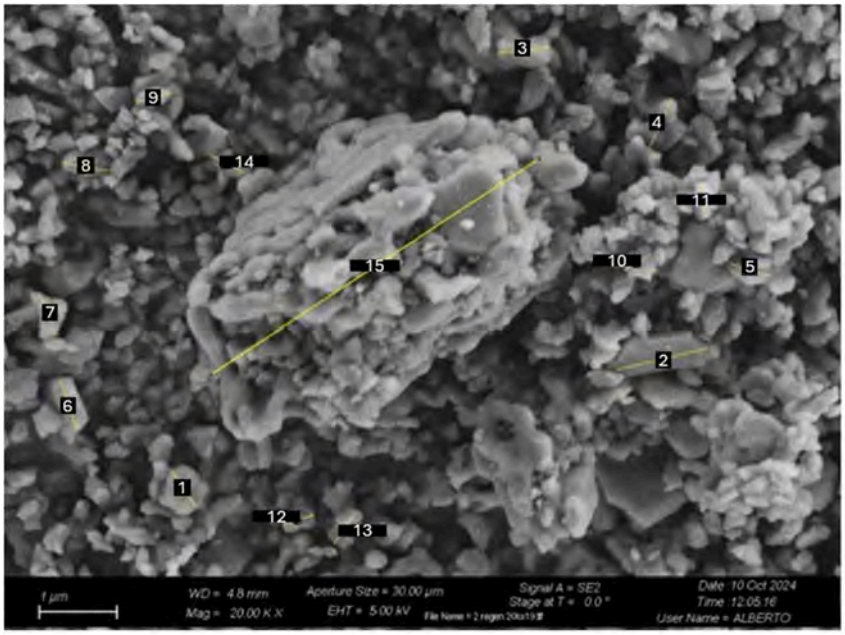

Label	Length (µm)
1	0,569
2	1,19
3	0,7
4	0,659
5	0,529
6	0,679
7	0,59
8	0,578
9	0,457
10	0,392
11	0,424
12	0,419
13	0,485
14	0,476
15	5,053

Fig. 7. SEM image of two-time recycled powder, with relative measurements.

Firstly, the sintered bodies were scanned with GOM Atos-Core (Carl Zeiss IQS Deutschland GmbH, Peine, Germany) 3D scanner. These samples were then tested using a shear tester machine (Xyztech, Panningen, Netherlands), that registered the breaking force for each of the 48 pins presented on the CharAM sample. The broken samples were scanned again, to get geometrical information about the breaking height and area. 3D scanning and breaking forces data were analysed through an already developed Python code, which outputs were the geometrical evaluation performed on the broken pins, the number of pins considered for the analysis, the Weibull statistic of breaking strength of the sample. The geometrical comparison was performed by the software considering the theorical dimensions reported in the Fig. 4.

Because of the presence of some brownish-reddish spots on the surface and inside the samples made of recycled materials, EDX and RFA (Bruker Tiger S8 WD-XRF, Bruker Corporation, Billerica, United States) analyses were performed, the former on the powders, the latter on the sintered samples, for investigating the reasons behind their presence.

3. Results

3.1. Powder characterizations

Initial powder, as well as one-time and two-time recycled powders, were analysed using SEM, and EDX, which was repeated on sintered samples too with no evident differences. Some of the performed SEM images are reported below (Figs. 5, 6, 7) showing that, comparing one time recycled Alumina with initial one, no agglomerates or non-grinded parts are present in the powder, and particles shape and dimensions are

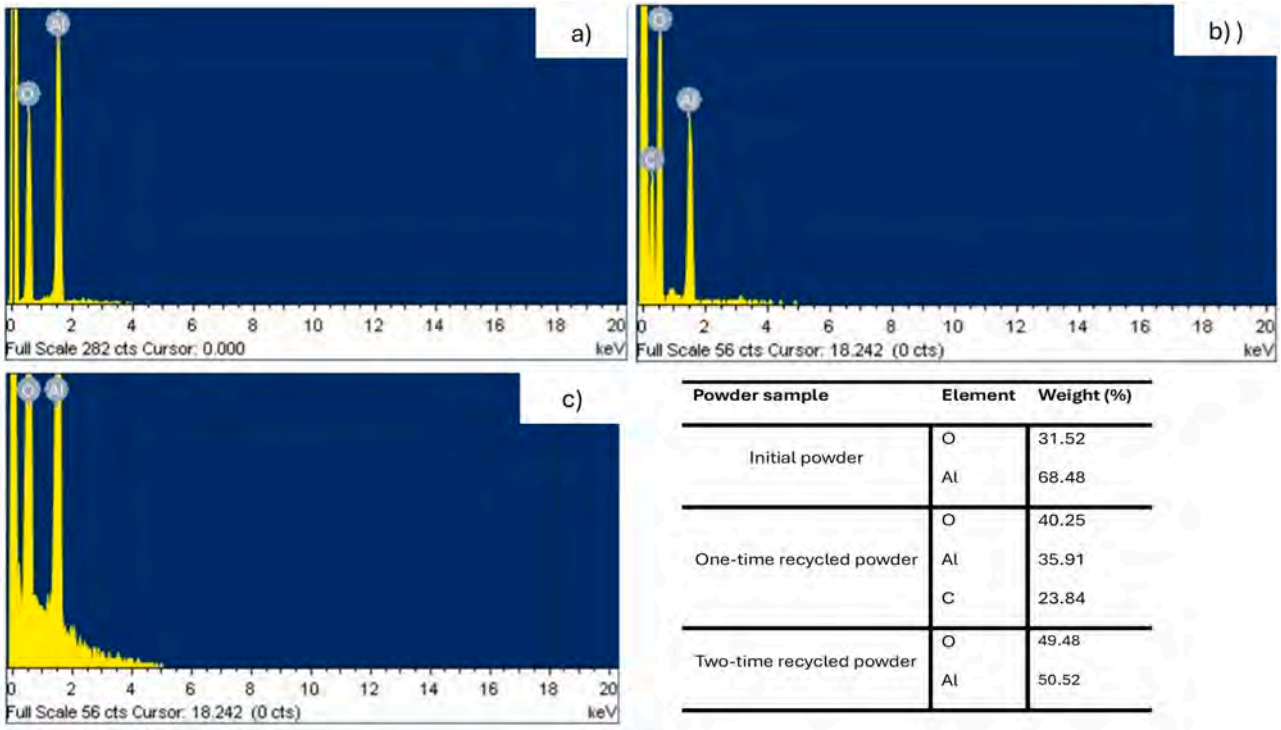

Powder sample	Element	Weight (%)
Initial powder	O	31.52
	Al	68.48
One-time recycled powder	O	40.25
	Al	35.91
	C	23.84
Two-time recycled powder	O	49.48
	Al	50.52

Fig. 8. EDX spectra of analysed samples: a) EDX spectrum of initial powder; b) EDX spectrum of one-time recycled material, with a carbon peak related to the used tape; c) EDX spectrum of two-time recycled material; d) EDX-related tables, divided by type of samples, that report the element weight percentage detected.

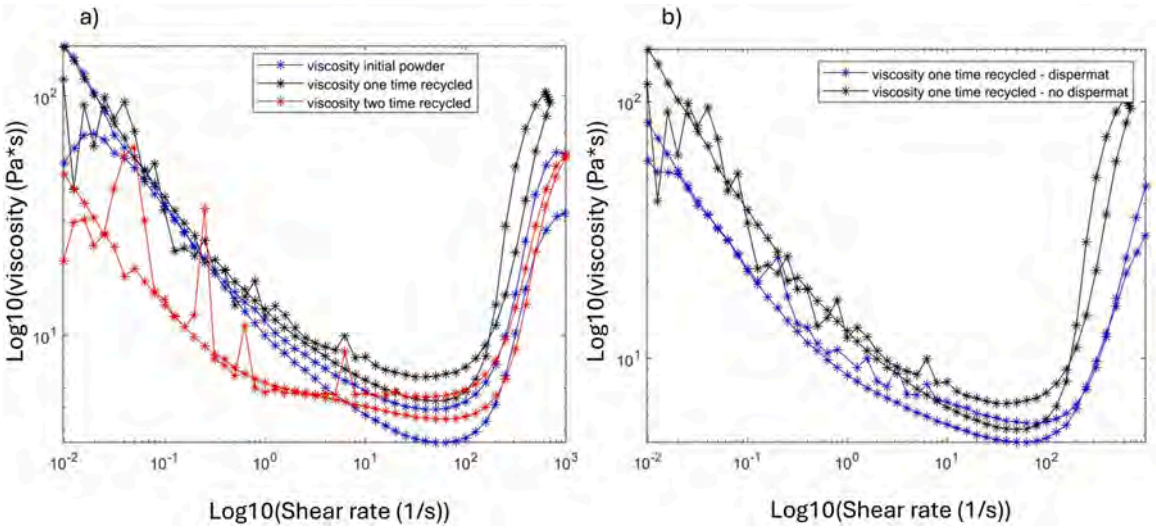

Fig. 9. Viscosity measurement performed: a) evaluation of the three samples; comparison before and after homogenization on one-time recycled alumina.

consistent. For two-time recycled powder, bigger particles and agglomerates can be seen in the SEM images. SEM images didn't prove big agglomerates, so no further investigations were performed on particles diameters.

The EDX analysis are reported in Fig. 8. Except for one peak in one-time recycled Al_2O_3, that is related to the carbon content of the used tape, no other materials peaks were detected, only Al and O peaks were observed. The relative weight percentages of aluminium and oxygen are reported in the table below, divided by samples.

3.2. Resins characterizations

Resin samples made of initial powder and recycled ones were used for viscosity measurement and curing depth of polymerized samples. Resins rheological behaviours are reported in the Fig. 9a. In the graph below there is a comparison of them, where lots of peaks are present in recycled materials. After mixing with the homogenizer the measurements were repeated, comparing one-time recycled powder resin before and after the homogenization (Fig. 9b).

Curing depth behaviour of the three samples is reported in the Fig. 10 below. The thicknesses obtained at each energy doses used for exposing the three resins are reported and compared, as showed in the graph, that highlights also how the measured thicknesses decrease at each recycling stage.

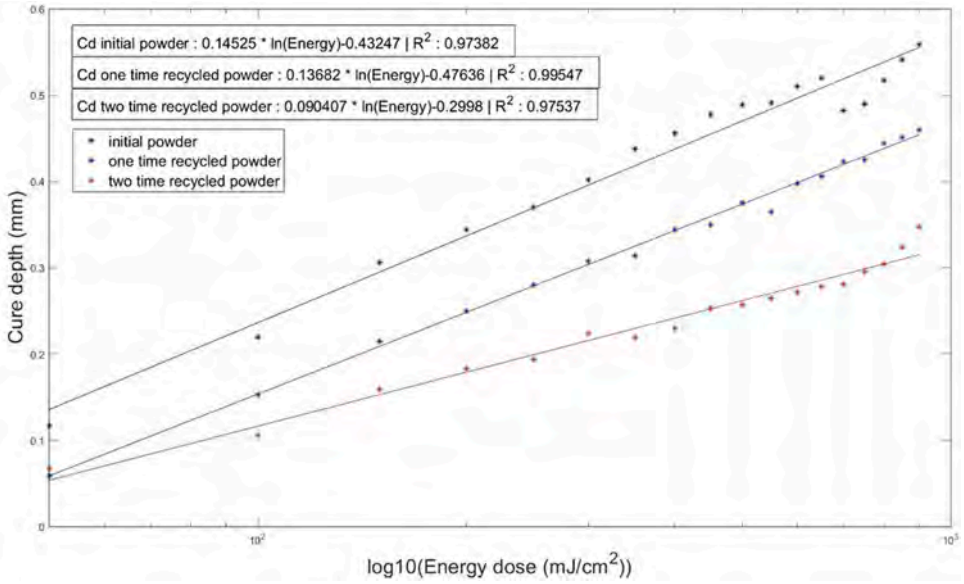

Fig. 10. Cure depth measurements of the three powder samples, with related linear regression formulas and R^2 values for reliability of the fitting curves.

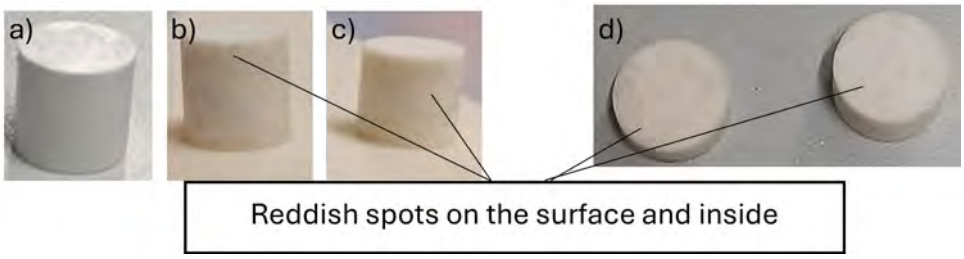

Fig. 11. Sintered sample from: a) initial powder; b) one-time recycled alumina; b) two-time recycled alumina. Redish spots appeared on the surface and inside cylinders made of recycled materials, as can be seen in the d) section of one-time recycled sample.

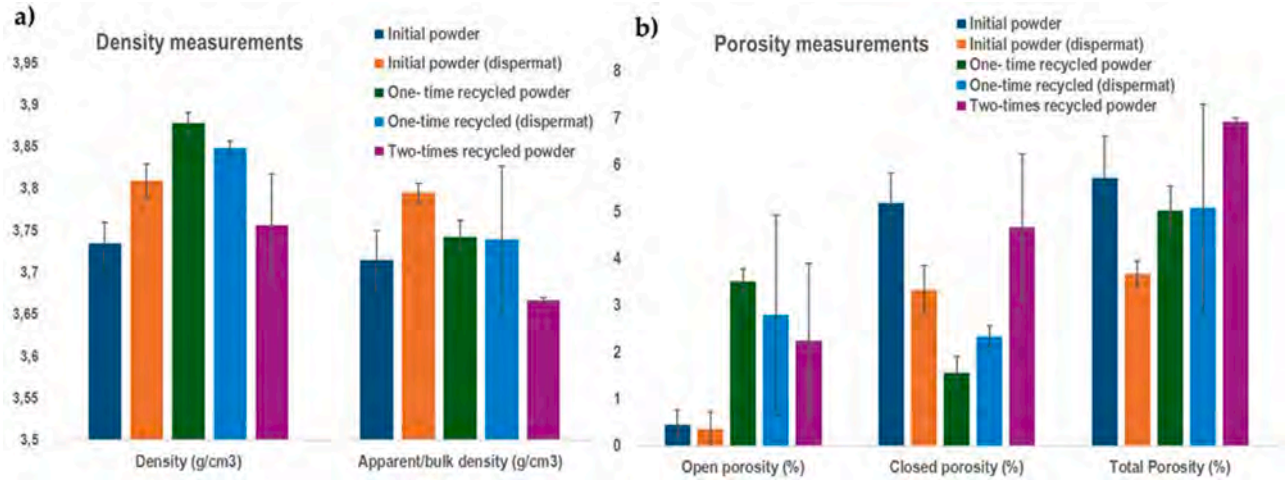

Fig. 12. Graph reporting: a) mean values and standard deviation bars of measured density for initial, one-time recycled and two-time recycled Al_2O_3 powder, before and after the use of homogenizer; b) mean values and standard deviation bars of the measured porosity, total, open and closed one.

3.3. Sintered body characterization

Sintered cylinders Fig. 11 were used for density evaluation through Archimedes' principle. The pictures show the presence of some reddish spots on the surfaces, that pushed the deeper investigation of powder through the RFA and EDX analysis, in order to evaluate the contaminants responsible for them. The measured density for initial, one-time recycled and two-time recycled alumina resins are in the Fig. 12 below. Together with density, material porosity was evaluated, and results are reported in the table too. Densities are quite in line in the three materials, but porosity is slightly higher in recycled samples, especially the total one in samples made of two-time recycled powder.

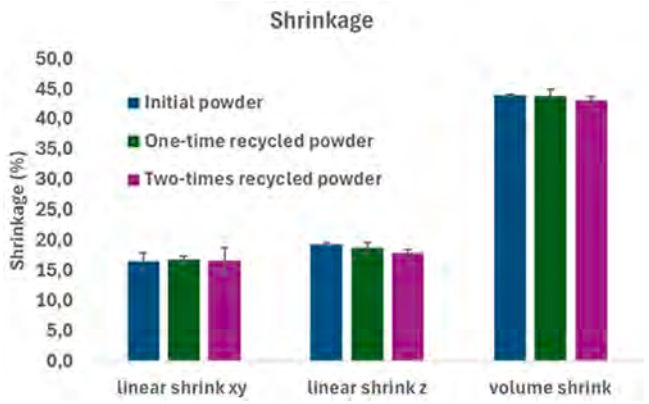

Fig. 13. Graph reporting linear and volumetric shrinkages mean values, as percentage, and standard deviation bars for the three batches of powder samples.

Cylinders like in the Fig. 11 were also fabricated for shrinkage evaluations, both in x- y- plane and z- axis, as also volumetric one, to check if the suggested shrinkage compensation factor is good for recycled materials too. As exposed in the below, the linear shrinkage in x- y- plane is consistent in the three materials, and it is about 16.8 %. Along z- axis, the value is around 19 % for initial and one-time recycled powders, and it is lower for two-time recycled one. Volumetric shrinkage is constant in initial and one-time recycled alumina, around 44 %, while it is lower in two-time recycled material (Fig. 13).

As already mentioned in the previous section (0 Samples characterization), the mechanical performance of the initial and recycled materials were evaluated through the CharAM methodology, applied on the sample in Fig. 14b. The sintered bodies (Fig. 15) were scanned, and the images were compared to the CAD files.

The scanning phase was then repeated for tested structures, to use the images for the CharAM program evaluation of geometrical features. Through them, it was possible to measure the width and thickness of the pins at different heights. Results of these measurements are reported below in Fig. 16. They showed that pins' width at different heights appeared consistent within the different tested samples, with few outliers and a narrow box, centred on the average value. The boxplots of pins' thickness at different heights instead showed a little discrepancy in the average values from 25 μm to 50 μm layer thickness samples, with some outliers especially in the new material graph. The performed measurements were repeated on samples made of alumina resin prepared with the use of homogenizer (Fig. 17). As for the case above, the boxplots of pins' width at different heights appeared consistent within the different tested samples, with no evident outliers, while in boxplots of pins' thickness at different heights more outliers could be seen, together with a little variation in the calculated average thickness values at different heights. Concerning the maximum strength at breaking

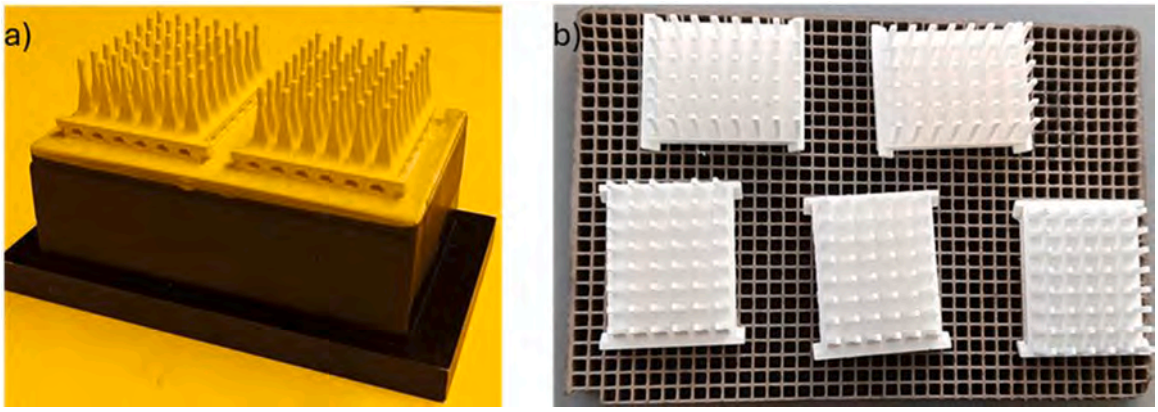

Fig. 14. Images of a) as-printed samples and b) sintered samples for CharAM testing methodology.

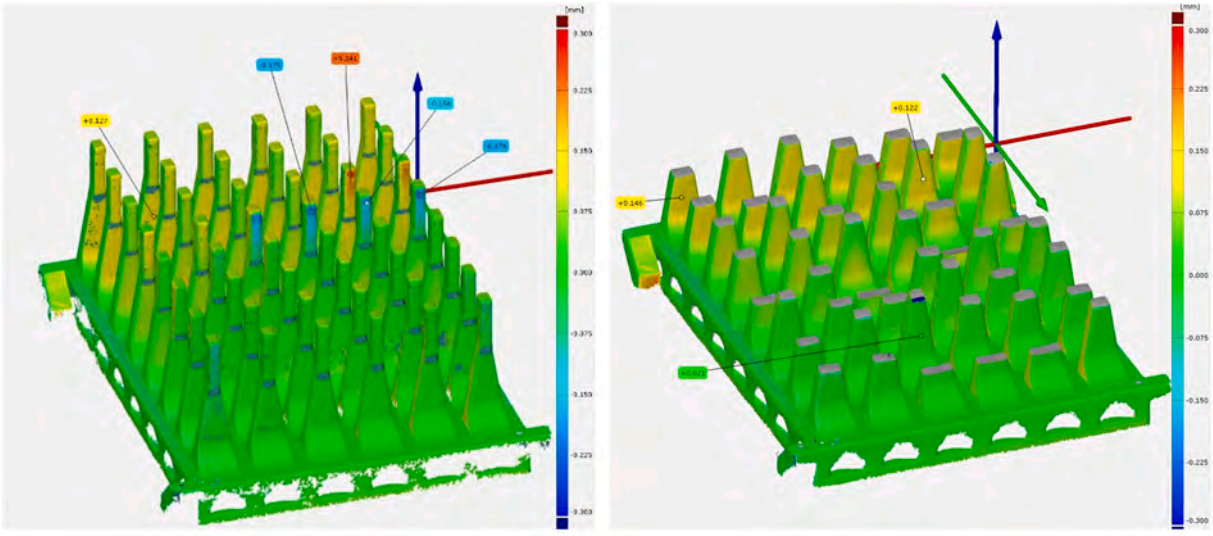

Fig. 15. 3D-Scan with surface comparison to CAD-file before (a) and after (b) CharAM testing.

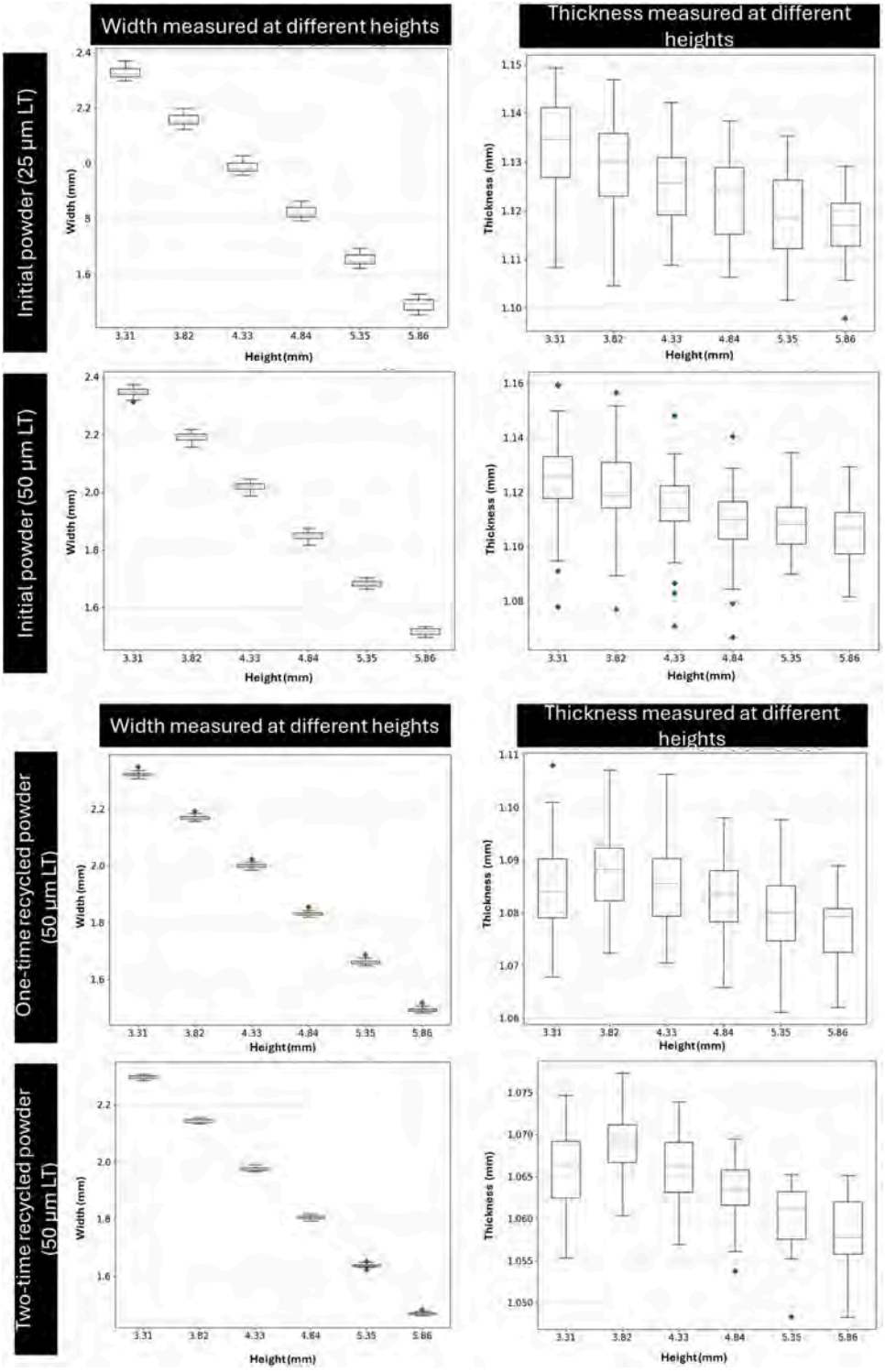

Fig. 16. Geometrical evaluations on samples made of first formulations, performed with already developed Python code.

point, the obtained data from the shear tester were elaborated, applying the Weibull statistical analysis, as reported in Fig. 18 and Table 3. Looking at graphs, they report the average strength, and the number of pins considered during the analysis, that means the number of valid inputs considered for the calculation. They also report the data fitting and the relative fitting equation, where the x variable coefficient is the calculated Weibull module. Except for the first graph (Fig. 18a), the Weibull modules are over 10, meaning that the distribution data is narrow shaped around the average calculated values. For both the new material and recycled ones (Fig. 18a-d), the measured strength was around 300 MPa (283.74 MPa for initial powder with LT of 25 µm, 309.26 MPa for initial powder with LT of 50 µm, 300.33 MPa for one-time recycled powder with LT of 50 µm), with a Weibull modulus greater than 10 for almost all the measurements made. Results of mechanical tests performed on homogenized resins' samples are reported in Fig. 18e-f, where the same trend was observed (348.95 MPa for new alumina), even if lower value was found for one-time recycled alumina compared to previous one (255.04 MPa).

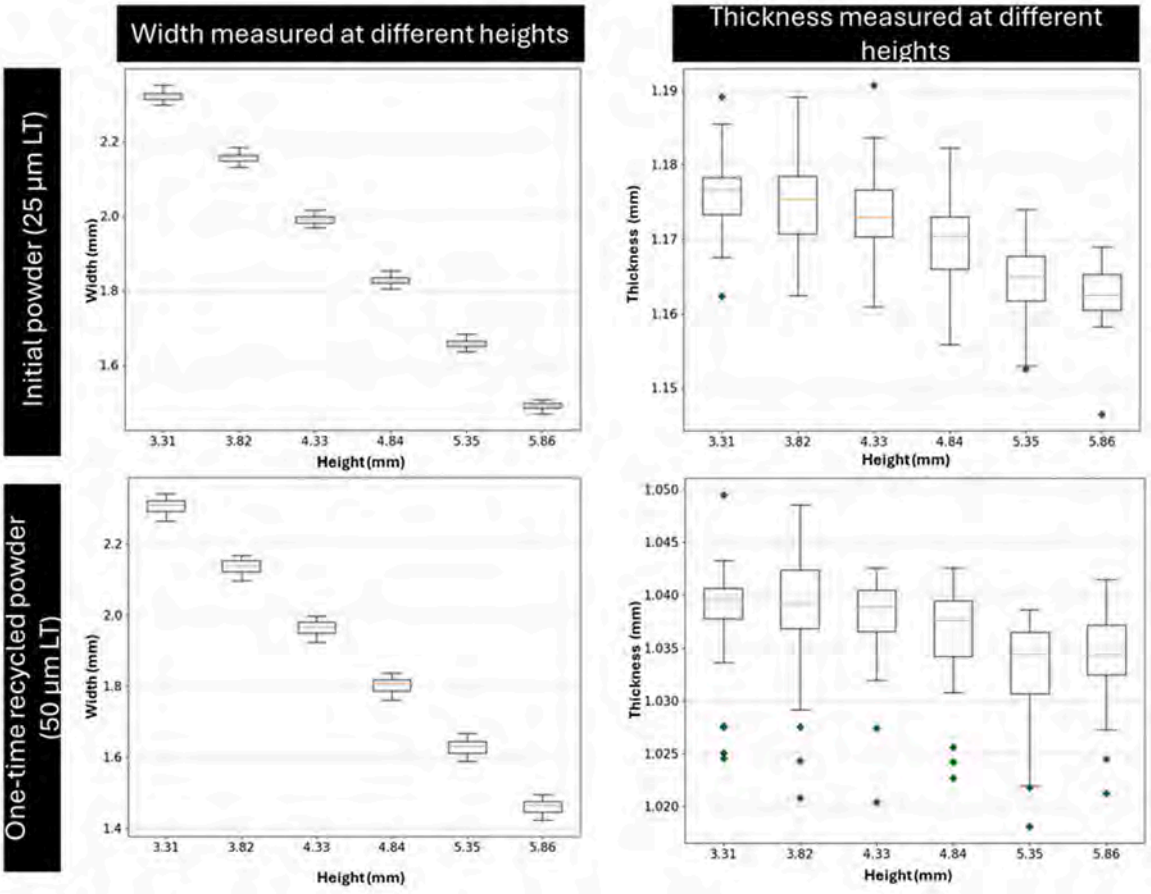

Fig. 17. Geometrical evaluations on samples made of homogenized resins, performed with already developed Python code.

Lastly, RFA was performed on the sintered samples made of the three different powders, to deeper investigate the contamination happened during the recycling process. The Table 4 below reports the mass percentage of each element found.

As shown in the table above, the initial material is not completely pure (99.7 % is the purity value indicated by the manufacturer and confirmed by the test), however some additional compounds were found in the recycled materials, with MgO appeared to be the most prominent one.

4. Discussion

This process is a first trial for reusing powder from printing errors and spare printed parts, however further evaluation of the environmental and economic impact of this process flow on powder is still to elucidate. The initial evaluation of the recycling procedure involved a comprehensive examination of the morphology and dimensionality of the obtained particles. To this end, SEM images were obtained. The comparison of SEM images revealed no big differences between one-time recycled material and initial alumina powder, nor were there any agglomerates or non-grinded parts observed. Furthermore, the absence of initial sintering necks was observed in the images, thereby confirming that the temperature employed during the burning process did not trigger any sintering activity, even though deeper analysis about the dimensionality of recycled material should be performed through particles size distribution. However, in two-time recycled powders, SEM images demonstrated some larger particles and agglomerates that could affect the resin properties as well as the mechanical behaviour of the final part. These agglomerates did not appear to be indicative of sintering activity, but their potential for disaggregation was likely due to additional grinding in the mixer stages. This disaggregating possibility was observed looking in the viscosity measurements performed (Fig. 9). Observing the curves of one-time recycled and two-time recycled alumina-based resins in particular, it is clear that the spikes in the first part of the curves, that arose in the beginning of the test phase, were no more observable in the returning phase of the curves, and if the same sample was used for more measurements, the behaviour was smoother. However, the observed spikes in the beginning of the curve were all under 20 s-1, that represents the starting shear rate for the used printing conditions. All through printing process, the shear rate increases, ensuring that non-linearities in viscosity measurement do not affect the results. In consideration of these observations, in conjunction with the impossibility of printing with a layer thickness of less than 50 µm, the additional process of homogenization was introduced in the preparation of resins. Because of preliminary tests results, demonstrating the poor performance of two times recycled alumina, deepen characterization, introducing the mentioned additional step for resin preparation, were pursued only for the more promising one time recycled alumina. The presence of small aggregates in the powdered materials probably hindered the correct photopolymerization during the printing process, as evidenced by the printing failure and the tortuous behaviour of the rheological curves. The effect of grains in the recycled materials was also observed during cure depth evaluation, as demonstrated by Fig. 10. The graph illustrated that as the powder type was changed from initial to one-time recycled and two-time recycled alumina, the measured thicknesses decreased at the same energy level, probably because of an increasing in scattering effects by the larger grains in recycled materials. This suggests that, when utilising recycled powder, it may be necessary to employ higher energy levels to achieve the desired layer thickness. The printed parts, after debinding and sintering, were used for density

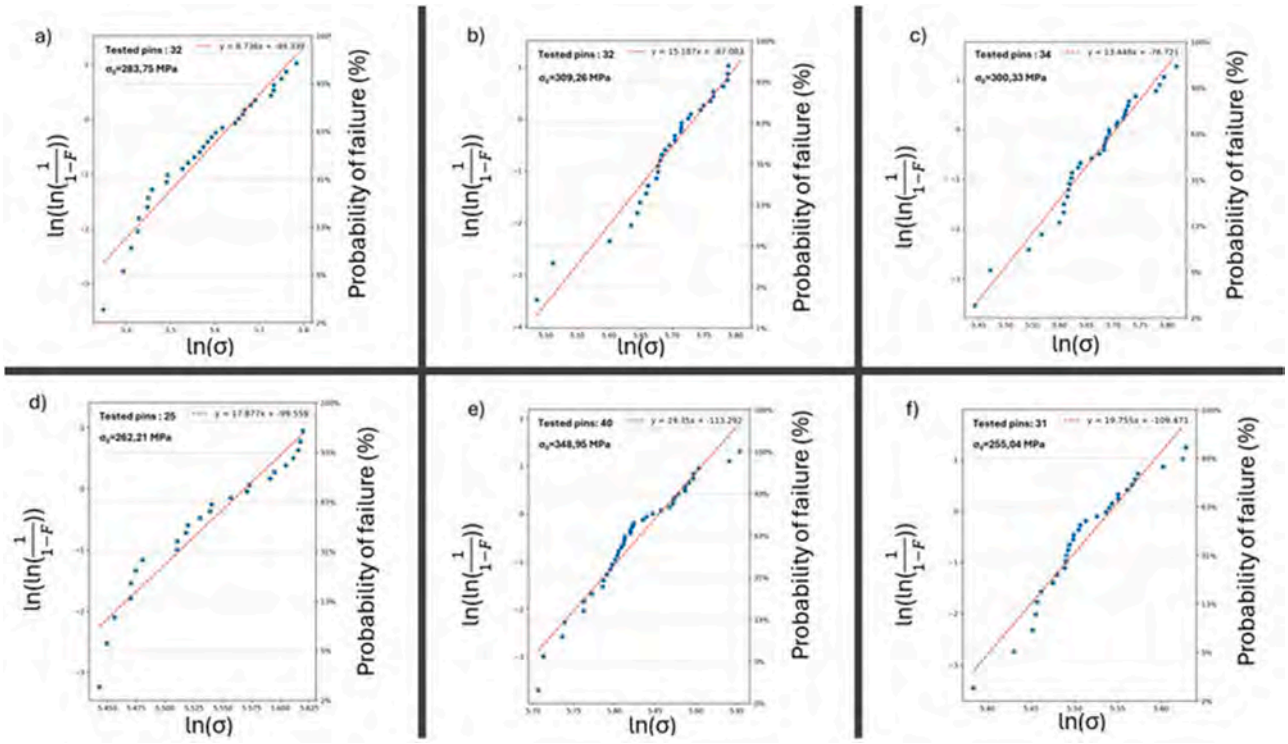

Fig. 18. Data analysis performed with Weibull statistics, to calculate the maximum strength of different materials, based on the already developed Python code: a) initial alumina samples, printed with 25 μm as layer thickness; b) initial alumina samples, printed with 50 μm as layer thickness; c) one-time recycled alumina samples, printed with 50 μm as layer thickness; d) two-time recycled alumina samples, printed with 50 μm as layer thickness; e) initial alumina samples, prepared using the homogenizer, printed with 25 μm as layer thickness; f) one-time recycled alumina samples, prepared using the homogenizer, printed with 50 μm as layer thickness.

Table 3
Resuming table, with the calculated values of strength, Weibull module and number of pins considered valid.

Sample name	Strength (MPa)	Weibull module – m	Num. pins
Initial powder (LT = 25 um)	283.75	8.74	32
Initial powder (LT = 50 um)	309.26	15.19	32
One-time rec (LT = 50 um)	300.33	13.45	34
Two-time rec (LT = 50 um)	262.21	17.88	25
Initial powder- homogenized (LT = 25 um)	348.95	19.35	40
One-time rec – homogenized (LT = 50 um)	255.04	19.75	31

Table 4
RFA results, the division is based on the samples type.

Samples type	Compound	Mass (%)
Initial powder	Al_2O_3	99.71
	SiO_2	0.23
	CaO	0.03
	Fe_2O_3	0.02
	Ga_2O_3	0.01
One-time recycled powder	Al_2O_3	98.90
	MgO	0.54
	SiO_2	0.23
	Cl	0.08
	SO_3	0.07
	TiO_2	0.05
	CaO	0.05
	K_2O	0.04
	Fe_2O_3	0.03
	Ga_2O_3	0.01
Two-time recycled powder	Al_2O_3	99.17
	MgO	0.49
	SiO_2	0.25
	Fe_2O_3	0.04
	Ga_2O_3	0.01
	NiO	0.01
	ZrO_2	58 PPM

measurement and porosity assessment, as well as for linear and volumetric shrinkage calculations. The one-time recycled material showed an internal density comparable to that of the initial alumina powder, although the total porosity was slightly higher than that of the new powder samples. This finding is consistent with the observed comparability of mechanical performances between CharAM samples fabricated using initial powder and those fabricated using one-time recycled powders. The investigation revealed that the one-time recycled material yield in the applied production process was consistent with the initial material, and no unusual deformation or variation in the pin area was observed. Samples fabricated from two-time recycled alumina exhibited higher porosity percentages and lower densities compared to the initial powder, which then matched the poorer mechanical performance observed in the CharAM test phase (261.21 MPa). Additionally, an anisotropic shrinkage behaviour could be appreciated in two time recycled alumina, due to the plausible bigger grains seen in SEM images, which made impossible to print part with a layer thickness below 50 μm, and showed lower active surfaces for sintering, strongly affecting the shrinkage of the parts too.

Furthermore, sintered samples from recycled materials presented some red spots on their surface, as well as in the interior. Consequently, RFA and EDX analyses were performed on these samples and their powder. EDX analysis revealed no evidence of contaminants, apart from some interference that was too low to measure and a 20 % carbon content in the one-time recycled material, attributed to the tape used to hold the powder in place. To obtain more precise results, RFA was employed to detect very low quantities of contaminants. A comparison

of the initial, one-time, and two-time recycled materials revealed the presence of significant quantities of composites from porcelain, like magnesium oxide, which can contribute to alumina pigmentation during the sintering stage [22,23]. The contamination is likely to have occurred during the recycling process, possibly due to the use of a mortar and pestle. This hypothesis was checked using AES11c initial powder for performing the same procedure applied to recycled material and saving small quantities of treated alumina at each step (thermal treatment, grinding, sieving step). Consequently, optimisation of the recycling process is essential, and further investigation into the cause is necessary.

5. Conclusion and future perspectives

The objective of this study was to develop a recycling process for all printing errors and excess components produced during the DLP fabrication of ceramic parts. The recovery of Al_2O_3 powder from the collected components was achieved by burning out the polymer matrix, grinding and sieving the obtained material. Subsequently, the recovered alumina was suspended in a photocurable resin, which was then used for printing. Throughout the process chain, a series of materials and components tests were conducted. Initially, a thorough investigation was conducted using SEM images and EDX analysis to determine whether the process had triggered the onset of sintering activity and whether any contamination had occurred during the recycling phase. A viscosity evaluation and cure depth measurement were performed on the resin to study its rheological behaviour and cure properties. Finally, sintered samples were utilized to evaluate density, mechanical performance and for RFA analysis. The findings of these tests demonstrated that the recycling process did not affect the final properties, including fracture strength, density, or particle size and morphology. This suggest the potential application of one-time recycled material for use cases where high strength and mechanical resistance are required. Furthermore, the implementation of the recycling process on already recovered powder has been shown to result in a decrease in the properties of the sintered bodies, suggesting that additional recycling steps could degrade the material. It is feasible to implement certain measures to reduce some of the mentioned problems, such as the introduction of an additional mixing phase through a homogenizer to disaggregate agglomerates. Future research might focus on the development of new recycling processes, whose main objective should be to avoid contamination of the powders and prevent their aggregation, or on the possibility of using other sources of alumina, perhaps from other manufacturing and finishing processes, in order to use DLP or other CerAM technologies to reintroduce these powders into the manufacturing chains. Exploration of the potential for reusing materials that have undergone two cycles of recycling, through their combination with new powder, should be undertaken. This should be accompanied by a Life Cycle Assessment (LCA) of the recycling process to assess the impact of the developed strategy. This preliminary approach to recycling ceramic materials for CerAM has the potential to serve as a framework for the development of reusing strategies for printing errors and brown bodies from more expensive and environmentally impactful materials, such as SiC, AlN, or Si_3N_4.

6. Summary of novel conclusions

The objective of this study is to demonstrate the feasibility of reusing alumina powder from DLP printing errors and excess components for CerAM VPP. SEM images showed that the recycling process did not trigger the onset of sintering activity, while EDX and RFA analyses reported no significant contamination that could affect properties, including fracture strength, density, or particle size and morphology, but only the appearance of the final objects.

Repeating the physical and mechanical characterization on samples made of one-time or two-time recycled alumina powder highlighted that one-time recycled material could still be used for cases where high strength and mechanical resistance are required. However, two-time recycled material showed in a decrease in the properties of the sintered bodies, suggesting that additional recycling steps could degrade the material.

This work could serve as a starting point for developing new strategies devoted to recycling ceramic materials through additive manufacturing techniques.

CRediT authorship contribution statement

Matilde Aronne: Writing – original draft, Resources, Methodology, Investigation, Formal analysis, Data curation, Conceptualization. **Eric Schwarzer-Fischer:** Writing – original draft, Resources, Methodology, Investigation, Formal analysis, Data curation, Conceptualization. **Alberto Ballesio:** Writing – review & editing, Investigation, Data curation. **Nadine Lorenz:** Writing – review & editing, Investigation, Data curation. **Valentina Bertana:** Writing – review & editing, Supervision. **Uwe Scheithauer:** Writing – review & editing, Project administration. **Sergio Ferrero:** Funding acquisition. **Luciano Scaltrito:** Writing – review & editing, Supervision, Project administration, Funding acquisition.

Declaration of competing interest

The authors declare that they have no known competing financial interests or personal relationships that could have appeared to influence the work reported in this paper.

Acknowledgment

This study was carried out within the MICS (Made in Italy—Circular and Sustainable) Extended Partnership, that received funding from the European Union Next-GenerationEU (NATIONAL RECOVERY AND RESILIENCE PLAN (NRRP)—MISSION 4 COMPONENT 2, INVESTMENT 1.3—D.D. 1551.11-10-2022, PE00000004). Special thanks to Dr. Chrisitan Berger, from Fraunhofer Institute für keramische Technologie und Systeme, for his support and suggestions in the reviewing phase of the current work.

Fundings: The work was partially supported by the research grant "SVINBO - SILICON VALLEY 8.0 IN Piedmont FOR A GREEN AND SMART MOBILITY funded by the Italian Ministry of Economic Development DM 09.12.2014 s.m.i. –Contratto di sviluppo" (CUP: C17J23000030001-CDS0000965).

References

[1] L.M. Rueschhoff, L.A. Baldwin, J.O. Hardin, J. Kaufman, Future directions in ceramic additive manufacturing: Fiber reinforcements and artificial intelligence, J. Am. Ceram. Soc. 107 (2024) 1505–1522, https://doi.org/10.1111/jace.19408.

[2] E. Fiume, B. Coppola, L. Montanaro, P. Palmero, Vat-photopolymerization of ceramic materials: exploring current applications in advanced multidisciplinary fields, Front. Mater. 10 (2023), https://doi.org/10.3389/fmats.2023.1242480.

[3] S. Zakeri, M. Vippola, E. Levänen, A comprehensive review of the photopolymerization of ceramic resins used in stereolithography, Addit. Manuf. 35 (2020) 101177, https://doi.org/10.1016/j.addma.2020.101177.

[4] S. Mamatha, P. Biswas, R. Johnson, Digital light processing of ceramics: an overview on process, materials and challenges, Prog. Addit. Manuf. 8 (2023) 1083–1102, https://doi.org/10.1007/s40964-022-00379-3.

[5] C.L Cramer, E. Ionescu, M. Graczyk-Zajac, A.T Nelson, Y. Katoh, J.J Haslam, L. Wondraczek, T.G Aguirre, S. LeBlanc, H. Wang, M. Masoudi, E. Tegeler, R. Riedel, P. Colombo, M. Minary-Jolandan, Additive manufacturing of ceramic materials for energy applications: Road map and opportunities, J. Eur. Ceram. Soc. 42 (2022) 3049–3088, https://doi.org/10.1016/j.jeurceramsoc.2022.01.058.

[6] E. Schwarzer-Fischer, U. Scheithauer, A. Michaelis, CerAMfacturing of aluminum nitride with high thermal conductivity via lithography-based ceramic vat photopolymerization (CerAM VPP), Ceramics 6 (2023) 416–431, https://doi.org/10.3390/ceramics6010024.

[7] H. Sun, B. Zou, X. Wang, W. Chen, G. Zhang, T. Quan, C. Huang, Advancements in multi-material additive manufacturing of advanced ceramics: A review of strategies, techniques and equipment, Mater. Chem. Phys. 319 (2024) 129337, https://doi.org/10.1016/j.matchemphys.2024.129337.

[8] H. Hegab, N. Khanna, N. Monib, A. Salem, Design for sustainable additive manufacturing: A review, Sustain. Mater. Technol. 35 (2023) e00576, https://doi.org/10.1016/j.susmat.2023.e00576.
[9] M. Javaid, A. Haleem, R.P. Singh, R. Suman, S. Rab, Role of additive manufacturing applications towards environmental sustainability, Adv. Ind. Eng. Polym. Res. 4 (2021) 312–322, https://doi.org/10.1016/j.aiepr.2021.07.005.
[10] M. Mehrpouya, A. Vosooghnia, A. Dehghanghadikolaei, B. Fotovvati, The benefits of additive manufacturing for sustainable design and production, Sustain. Manuf. (2021) 29–59, https://doi.org/10.1016/B978-0-12-818115-7.00009-2.
[11] H. Jayawardane, I.J. Davies, J.R. Gamagec, M. Johna, W.K. Biswas, Sustainability perspectives – a review of additive and subtractive manufacturing, Sustain. Manuf. Serv. Econ. 2 (2023).
[12] A. Al Rashid, M. Koç, Additive manufacturing for sustainability and circular economy: needs, challenges, and opportunities for 3D printing of recycled polymeric waste, Mater. Today Sustain. 24 (2023) 100529, https://doi.org/10.1016/j.mtsust.2023.100529.
[13] Alumina Price: Charts, Forecasts & News - FocusEconomics n.d. https://www.focus-economics.com/commodities/base-metals/alumina/(accessed April 9, 2025).
[14] Ju Y. Production cost rise is a concern for alumina refining in China as downturn deepens - Fastmarkets 2022. https://www.fastmarkets.com/insights/production-cost-rise-is-a-concern-for-alumina-refining-in-china-as-downturn-deepens/(accessed April 9, 2025).
[15] Aronne M., Schwarzer-Fischer E., Bertana V., Mossotti G., Scheithauer U., Ferrero S., Scaltrito L. Exploring circularity in ceramic 3D printing: possibilities and implementation. Under Submission 2025.
[16] Ceramic Manufacturing Industry | EU-BRITE n.d. https://eippcb.jrc.ec.europa.eu/reference/ceramic-manufacturing-industry (accessed April 9, 2025).
[17] M. Staudacher, U. Scheithauer, M. Reichel, N. Lorenz, M. Schwentenwein, T. Lube, Strength testing of additive manufactured ceramics – A round robin using the CharAM-methodology, Open Ceram. 17 (2024) 100557, https://doi.org/10.1016/j.oceram.2024.100557.
[18] M. Staudacher, T. Lube, J. Glettler, U. Scheithauer, M. Schwentenwein, A novel test specimen for strength testing of ceramics for additive manufacturing, Open Ceram. 15 (2023) 100410, https://doi.org/10.1016/j.oceram.2023.100410.
[19] E. Schwarzer-Fischer, U. Scheithauer, A. Michaelis, CerAMfacturing of aluminum nitride with high thermal conductivity via lithography-based ceramic vat photopolymerization (CerAM VPP), Ceramics 6 (2023) 416–431, https://doi.org/10.3390/CERAMICS6010024. Pages2023;6:416–31.
[20] K. Wang, M. Qiu, C. Jiao, J. Gu, D. Xie, C. Wang, X. Tang, Z. Wei, L. Shen, Study on defect-free debinding green body of ceramic formed by DLP technology, Ceram. Int. 46 (2020) 2438–2446, https://doi.org/10.1016/J.CERAMINT.2019.09.237.
[21] Y. Chen, J. Tan, J. Sun, H. Guo, J. Bai, P. Zhou, D. Zhang, G. Liu, Effect of sintering temperature on the microstructures and mechanical properties of ZrO2 ceramics fabricated by additive manufacturing, Ceram. Int. 50 (2024) 11392–11399, https://doi.org/10.1016/J.CERAMINT.2024.01.039.
[22] N. Tamsu Selli, Relationship between microstructure and the impact resistance of porcelain stoneware tiles, Bol. Soc. Esp. Cerám. Vidr. 61 (2022) 210–219, https://doi.org/10.1016/j.bsecv.2020.10.001.
[23] Causes of spots on the surface of alumina ceramics - ZC-TECH n.d. https://www.zc-newmaterials.com/causes-of-spots-on-the-surface-of-alumina-ceramics/(accessed April 15, 2025).